Oligomerization of the EGF Receptor Investigated by Live Cell Fluorescence Intensity Distribution Analysis

Saveez Saffarian,* Yu Li,‡ Elliot L. Elson,† and Linda J. Pike†
*Department of Cell Biology, Harvard Medical School, Boston, Massachusetts 02155; and †Department of Biochemistry and Molecular Biophysics, and ‡Department of Physics, Washington University School of Medicine, St. Louis, Missouri 63110

ABSTRACT Recent evidence suggests that the EGF receptor oligomerizes or clusters in cells even in the absence of agonist ligand. To assess the status of EGF receptors in live cells, an EGF receptor fused to eGFP was stably expressed in CHO cells and studied using fluorescence correlation spectroscopy and fluorescent brightness analysis. By modifying FIDA for use in a two-dimensional system with quantal brightnesses, a method was developed to quantify the degree of clustering of the receptors on the cell surface. The analysis demonstrates that under physiological conditions, the EGF receptor exists in a complex equilibrium involving single molecules and clusters of two or more receptors. Acute depletion of cellular cholesterol enhanced EGF receptor clustering whereas cholesterol loading decreased receptor clustering, indicating that receptor aggregation is sensitive to the lipid composition of the membrane.

INTRODUCTION

The EGF receptor is a classical plasma membrane receptor tyrosine kinase. It is composed of three distinct domains: i), an extracellular domain that binds EGF; ii), a transmembrane domain that spans the membrane once as an α-helix; and, iii), a cytoplasmic domain that possesses tyrosine kinase activity (1). In the traditional model of EGF receptor activation (2), the EGF receptor exists as a monomer that is held in a tethered, inactive configuration by intramolecular interactions (3). Upon stimulation with EGF, these intramolecular interactions are broken and the protein adopts an open configuration that permits back-to-back dimerization of two EGF monomers (4,5). This leads to the activation of the intracellular tyrosine kinase activity and the autophosphorylation of the EGF receptor. These phosphotyrosines serve as docking sites for the binding of proteins to the EGF receptor and the complexes thus formed initiate a cascade of events that ultimately culminates in cell proliferation.

The entire chain of events that follows the binding of EGF to its receptor begins with the dimerization of the EGF receptor. Although it is generally believed that the inactive form of the receptor is a monomer and the active form is a dimer, recent evidence suggests that this model may not be complete. Moriki et al. (6) showed by chemical cross-linking that a majority of the EGF receptors expressed in B82 cells existed as dimers in the absence of EGF. Using FRET and/or FLIM, Gadella and Jovin (7) and Martin-Fernandez et al. (8) reported that a significant fraction of EGF receptors were oligomerized before EGF binding. Similarly, Sako et al. (9) used single-molecule imaging techniques to show that singly ligated EGF receptor dimers existed in intact cells. More recently, Clayton et al. (10) used image correlation microscopy and FRET to show that before ligand binding, EGF receptors existed in clusters containing an average of ~2 receptors but that cluster size increased to ~4 after treatment with EGF. Thus, the EGF receptor system appears to involve more than a simple monomer-dimer equilibrium. But whereas previous studies have provided some insight into the oligomerization of the EGF receptor, the methods employed in these studies required the use of nonphysiological conditions, such as cell fixation or low temperatures. Thus, it is not clear that the results accurately reflect the behavior of the EGF receptor under more biologically relevant conditions. In addition, the methods yield values only for the population average in terms of receptor clustering rather than providing explicit information on the fraction of receptors that exists in clusters of a particular size.

Despite the general importance of receptor oligomerization and protein-protein interactions in cell signaling events, few methods are available to study such interactions at the single molecule level in live cells. We have therefore developed a modified approach to FIDA that permits the assessment of membrane protein clustering in live cells under physiological conditions. The approach is specifically tailored for use with membrane proteins fused to a fluorescent reporter molecule and diffusing in the plane of the plasma membrane.

The brightness of any fluorophore (i.e., the number of photons emitted per second per fluorophores at a given level of excitation) is an intrinsic molecular property of that molecule. The total brightness of any group of fluorophores is the

Submitted January 29, 2007, and accepted for publication March 27, 2007.

Saveez Saffarian and Yu Li contributed equally to this work.

Address reprint requests to Linda J. Pike, E-mail: pike@biochem.wustl.edu.

Abbreviations used: BS^3, bis(sulfosuccinimidyl)suberate; BSA, bovine serum albumin; EGF, epidermal growth factor; eGFP, enhanced green fluorescent protein; FCS, fluorescence correlation spectroscopy; FIDA, fluorescence intensity distribution analysis; FLIM, fluorescence lifetime imaging microscopy; FRET, fluorescence resonance energy transfer; PCH, photon count histogram.

Editor: Brian R. Dyer.

0006-3495/07/08/1021/11 $2.00 doi: 10.1529/biophysj.107.105494

sum of the individual molecular brightnesses in the absence of any electronic interactions among the fluorophores. Thus, brightness can be used to quantify the number of molecules moving together in a group.

Several theoretical methods have been developed for the analysis of the brightness of molecules diffusing in solution. Brightness analysis began with the analysis of the moments of the fluorescence intensity (11,12). Two later approaches, involving analysis of the photon count histogram, expanded the type of information that could be obtained from the brightness analysis. The photon count histogram can be directly analyzed using curve fitting approaches with one or multiple brightnesses as the free parameters in the fit. This method, termed PCH analysis, was pioneered by Chen and colleagues and has been shown to be a very powerful tool for the analysis of the brightnesses of molecules in the cellular environment (13–16). However, PCH analysis has so far provided information only on the average brightness of molecules in a distribution, not the distribution of brightnesses. FIDA, a mathematically equivalent approach, utilizes inverse transforms to directly yield the distribution of the brightnesses from the distribution of the photon counts (17). In principle, both PCH and FIDA are capable of providing information on the distribution of brightnesses. However, this requires a large set of free parameters in the fitting which in turn necessitates high photon counts for accurate analyses. As a result, the application of such brightness analyses to live cells has been limited, largely due to the damage caused by the high laser intensities required to generate sufficiently high photon counts.

Here, we introduce a few simplifications in FIDA that make it suitable for use in living cells, and importantly, allow the extraction of explicit information on the distribution of fluorescent molecules among clusters of increasing size. We take advantage of the fact that the allowable brightness values must be integer multiples of the brightness of eGFP. This significantly reduces the number of free parameters and hence the requirement for high photon counts. This modified FIDA can be used to assess the state of oligomerization of membrane proteins in whole cells.

We have applied this method to study the clustering of eGFP-labeled EGF receptors in cells. The analysis indicates that under control conditions, the EGF receptor exists as a heterogeneous population of clustered species. The majority of receptors exist as single molecules, however clusters containing two or four receptor molecules are also present. Surprisingly, depletion of cholesterol increases the clustering of the EGF receptor whereas cholesterol loading converts the receptors to an almost entirely monomeric population. These findings are corroborated by chemical cross-linking studies which show an increase in receptor oligomers after cholesterol depletion and a decrease in oligomers after cholesterol loading. EGF-stimulated receptor autophosphorylation was enhanced in the more highly clustered, cholesterol-depleted cells and inhibited in the monomeric, cholesterol-loaded cells. These data are consistent with the existence of a sizable population of EGF receptor clusters in unstimulated cells and suggest that the extent of EGF receptor clustering depends on cellular cholesterol levels. Furthermore, the data suggest that the strength of the output signal from the EGF receptor is modulated by a preexisting equilibrium among clustered species.

MATERIALS AND METHODS

Materials

Methyl-β-cyclodextrin was obtained from Fluka Chemical (Buchs, Switzerland). The polyclonal anti-EGF receptor antibody was from Santa Cruz (Santa Cruz, CA). The anti-phosphotyrosine antibody, PY20, was from B-D Biosciences (Palo Alto, CA). Immobilon-P was from Millipore (Billerica, MA).

Cells and tissue culture

Tissue culture

CHO cells were cultured at 37°C in Ham's F12 medium containing 10% fetal calf serum in a 5% CO_2 humidified incubator. A construct in peGFP-N1encoding the EGF receptor C-terminally fused to E-GFP was transfected into CHO cells and stable transfectants isolated by growth in G418. For FCS experiments, cells were plated onto two-well glass slide chambers 48 h before use and refed 16 h before the experiment. Before FCS experiments, cells were washed and transferred into warmed Hepes-buffered saline solution containing 25 mM Hepes, pH 7.2, 120 mM NaCl, 5 mM KCl, 5 mM $MgCl_2$, 1 mM $CaCl_2$, 2 mg/ml glucose and 1 mg/ml BSA. During the experiments, cultures were maintained at 37°C by placing the glass slide chambers on a heated stage (Zeiss, Thornwood, NY).

Cholesterol depletion or loading

Cells were depleted of cholesterol by treatment for 30 min at 37°C with 10 mM methyl-β-cyclodextrin in serum-free Ham's F12 medium containing 25 mM Hepes, pH 7.2 and 1 mg/ml BSA. Cells were loaded with cholesterol by treatment for 30 min at 37°C with 0.2 mM cholesterol/methyl-β-cyclodextrin complexes in the same medium (18).

Cross-linking of EGF receptors

CHO cells expressing EGF receptors were grown in 35 mm wells and depleted or loaded with cholesterol as described above. The treatment media was removed and replaced with Hanks' balanced salt solution containing 5 mM $MgCl_2$ and 1 mM $CaCl_2$. Cells were treated with or without 25 nM EGF in the absence or presence of 10 mM BS^3 for 15 min at 25°C. The medium was removed and replaced with medium containing 20 mM glycine to quench the reaction. Lysates were then prepared in RIPA buffer as described (19). Proteins were separated on a 5% SDS polyacrylamide gel and Western blotted for EGF receptors.

EGF receptor autophosphorylation assays

Cells were grown in 35 mm dishes and depleted or loaded with cholesterol as outlined above. The medium was removed and replaced with 1 ml of Ham's F12 medium containing 25 mM Hepes, pH 7.2 and 1 mg/ml BSA plus 25 nM EGF. Cells were incubated for 2 min at 37°C. The medium was removed and lysates prepared in RIPA buffer as described (19); 50 μg protein from each lysate was loaded on a 9% SDS polyacrylamide gel and proteins separated

by electrophoresis. Proteins were transferred electrophoretically to Immobilon-P and Western blotted for EGF receptor or phosphotyrosine (19).

FCS and FIDA Analysis

Instrumentation

FCS experiments were performed on a LSM 510 ConfoCor 2 Combination System from Carl Zeiss Germany. The instrument is fully motorized and controlled through a standard high-end Pentium PC. The system is based on a Zeiss Axiovert 200M inverted microscope. A water immersion C-Apochromat 40× objective (numerical aperture 1.2) focused the excitation light in a diffraction-limited mode. The pinhole size was 70 μm. The collimated fluorescence was reflected by a mirror and focused onto an avalanche photodiode unit. Some early data were obtained using a home-built system previously described (20). Data obtained using this system were comparable to those obtained using the Confocor 2.

A test Alexa 488 sample in a phosphate buffer was used for calibration of the beam profile. The brightness of the Alexa 488 dye was calculated and used to check the stability of the instrument during long experiments. All the data analysis was performed using Origin software (Originlab) and home-developed Labview and MatLab programs.

Laser intensity was measured by attaching the detector of a high-sensitivity power meter (LaserMate-Q, Coherent) over a 20× infinity-corrected air objective. Laser power was 5.4 mW in all experiments. As shown in Supplemental Fig. 1, this value is within the range in which there is no apparent optical saturation of eGFP.

Measurements and data analysis

Initially, a Z-scan was performed to locate the apical and basal membranes. Only one measurement from each membrane was taken per cell. The results obtained were independent of which membrane was used for data acquisition. Thus, all data sets were pooled in the final analysis.

After positioning the laser beam on the membrane based on the Z-scan, the fluorescence intensity reached a steady state in 10 s. During this period, immobile receptors likely undergo slow photobleaching and so contribute little to the FCS or PCH measurements. A 100-s fluorescence trace was acquired from which both correlation function and PCH were calculated. For the correlation function, the fluorescence trace was parsed into ten 10-s traces. From each 10-s trace, a correlation function was calculated and the average of these correlation functions was fit to Eq. 11 below using Origin software. The experimental standard error was determined for each point of the correlation function. These errors were used to weight the data during the fitting and error analysis of the sample (20,21). Goodness of fit was determined by chi-square analysis. Chi-square values ranged from 0.53 to 1.12. Representative PCH curves and fits with their corresponding residual analyses are presented in Supplemental Fig. 2.

The PCH was calculated from the 100-s trace using a bin time of 4.0 ms. Using a home-written MatLab routine, the fast Fourier transform of the PCH was calculated and fit using Eq. 9 with the q grid (q, $2q$, $4q$, $8q$) as described in Results. Equation 9 was reformatted to match MatLab's definition of the fast Fourier transform. Background fluorescence was measured in the interior of the cell far enough from the cell surface to minimize contributions from membrane-bound eGFP and was generally $<10\%$ of the total fluorescence (see Z-scan in Supplemental Fig. 3). The background fluorescence for each measurement was taken into account in the MatLab routine that fit the logarithm of the Fourier transform of the experimental PCH to Eq. 9. Changing the background by a factor of 2 had little effect on the outcome of the analysis.

Although the brightness values are linked through the grid, each experiment produces four brightness values and four corresponding concentrations. The total concentration of clusters from each cell was normalized to one before the brightness histogram was generated. The measurement of more than 30 spots on the plasma membrane produced ~120 brightness values with corresponding concentrations. A histogram was then created from these data. To do this, the concentrations of all the species with brightness values within a window of brightnesses were summed and then presented as a point in the histogram at the average value of brightness for that window. The windows in which the brightnesses were summed were: 0–2, 2–4, 4–6, 6–8, 8–10, 10–12, 12–16, 16–20, 20–24, 24–28, and 28–32 kHz. The corresponding average brightness values for these windows were: 1, 3, 5, 7, 9, 11, 14, 18, 22, 26, and 30 kHz.

In silico error analysis

To analyze the error of the PCH, a theoretical PCH curve was first generated by inverting the Fourier transform in Eq. 10 below. The noise associated with a finite experiment time is Poissonian and has been previously described (14). Attempting to assess error by adding random noise to the PCH curve, however, results in artifacts of normalization as well as negative values in the PCH. To avoid these problems, we have simulated the effects of limited data acquisition time on the amount of noise in a PCH. Using the theoretical PCH as a probability function, we have simulated a fluorescence trace over a defined time. A PCH that includes the Poissonian noise was then generated from this finite fluorescence trace. Each of the in silico experiments was repeated with a different seed of random numbers five times and the resulting brightnesses were then histogrammed as described above.

RESULTS

The theory of modified fluorescent intensity distribution analysis

As they pass through a confocal excitation volume, fluorescent molecules are excited by the laser beam and their fluorescence is captured. The number of photons registered during a predefined time window called the bin time, is counted and plotted versus time to create the fluorescence trace of the sample. The bin time is set to one-tenth the diffusion time of the molecule under study, so that the molecular motion during each bin time is small. The photon count histogram (PCH) is the probability of detecting a certain number of photons during the chosen bin time in the fluorescence trace.

Brightness, q, is a combination of molecular and instrumental specifications defined below:

$$q = \lambda B_0. \tag{1}$$

λ is a product of absorption cross section, quantum efficiency of the molecule and the detection efficiency of the microscope. B_0 is the maximum laser intensity in the focal plane of the laser. When the instrumental factors are constant, the brightness depends only on molecular spectroscopic properties.

The statistics of the PCH depend strongly on the average number of photons detected per molecule per bin time, which is equal to the brightness multiplied by the bin time. Hypothetically, if one had an excitation volume the size of the fluorescent molecule with an almost infinite fluorescence emission, then the photon count histogram would be identical to the distribution of fluorescence brightnesses of the sample. In reality, brightness is limited and the confocal volume is much larger than the size of the molecule so that a

number of fluorescent molecules can be in the volume at one time. This volume can be defined by $B(r)$, where B is the combination of laser excitation and fluorescence detection efficiency normalized so that $B(0) = 1$ and is ideally a three-dimensional Gaussian.

Following the derivation of Kask et al. (17) for this section, we divide $B(r)$ into subsets of equal intensity regions called B_i, which correspond to annular areas, dV_i, in the sample. The probability of registering n photons from a section of the beam characterized with B_i and volume dV_i can be written as a convolution of two Poissonian processes, one corresponding to the occupation number fluctuation and the other, the shot noise from the detector (17)

$$P_i(n) = \sum_{m=0}^{\infty} \frac{(cdV_i)^m}{m!} e^{-cdv_i} \frac{(mqB_iT)^n}{n!} e^{-mqB_iT} \quad (2)$$

for a species at molar concentration c, where $T =$ bin time.

A generating function can be defined as follows:

$$G(\xi) = \sum_{n=0}^{\infty} P(n)\xi^n. \quad (3)$$

By putting Eq. 2 into Eq. 3, and doing some algebra, one can get the representation of the generating function for the distribution of clusters of different brightness denoted by the index, j:

$$G(\xi) = \exp\left(\sum_j c_j \int_V \{\exp[(\xi - 1)q_jB(r)T] - 1\}dV\right). \quad (4)$$

Since we are interested in the clustering of eGFP fused to molecules diffusing in the membrane, we can tailor the analysis to our problem. We start by rewriting the problem strictly in two dimensions. This obviates the need for the costly correction of the observation volume in z (the optical axis) (14,17) and the laser profile can be well-approximated to a Gaussian ($B(r) = B_0e^{-2r^2/w^2}$) in the focal plane of the laser:

$$F(q_j, \xi) = \int_0^{\infty} \{\exp[(\xi - 1)q_je^{-2r^2/w^2}TB_0] - 1\}2\pi r dr \quad (5)$$

$$G(\xi) = \exp\left(\sum_j c_jF(q_j, \xi)\right). \quad (6)$$

By setting $\xi = e^{i\upsilon}$, the generating function becomes the Fourier transform:

$$G(e^{i\upsilon}) = \sum_{n=0}^{\infty} P(n)e^{i\upsilon n} = FT(P, \upsilon) \quad (7)$$

$$f(q_j, \upsilon) = \int_0^{\infty} \{\exp[(e^{i\upsilon} - 1)q_je^{-x}TB_0] - 1\}dx \quad (8)$$

$$FT(P, \upsilon) = \exp\left(\sum_j N_jf(q_j, \upsilon)\right) \quad (9)$$

$$Ln(FT(P, \upsilon)) = \sum_j N_j(f(q_j, \upsilon)) \quad (10)$$

$$N_j = C_j\frac{\pi\omega^2}{2}.$$

The left side of Eq. 9 is the Fourier transform of the experimental PCH. Since the functional forms of the f functions are known (Eqs. 5 and 8), one can fit the right side of Eq. 10 to the experimentally determined left side while varying the subset of N and q variables.

In the derivation of FIDA, a large subset of constant q parameters is considered and the best fit is obtained by changing the distribution of N while maintaining some regularization principles. Although this approach is powerful, due to the large subset of q parameters, it requires high photon counts per molecule. High photon counts per molecule can be achieved by increasing the laser intensity in solution experiments but this would lead to fast photobleaching in cellular experiments. On the other hand, one or two free floating brightness values can be fitted to the histogram using a traditional fitting mechanism but this approach provides little information beyond the average brightness of the sample (13,15,16,22).

In our experiments, each EGF receptor is fused to one eGFP molecule. Thus, for our analysis, we have made the simplifying assumption that aside from the background, the brightness values in each experiment should be multiples of the eGFP brightness. Thus, instead of generating a vast brightness map, we use the following grid: q, $2q$, $4q$, and $8q$. In the fitting procedure, both q and the corresponding concentrations of each species at a given brightness are free to be determined by the algorithm. We have observed experimentally that the width of the PCH is proportional to the square root of the brightness (not shown). Hence, this approach ensures approximately equal significance of the selected brightness grid points and quantization of the eGFPs on the cell membrane.

It is important to note that, although the average value of the eGFP brightness on the membrane can be calculated, it can not be used as a fixed parameter. The eGFP brightness in each experiment depends on the azimuthal positioning of the beam on the membrane and varies slightly among experiments.

Estimating the eGFP brightness on the membrane

The instantaneous molecular brightness of eGFP fluctuates between bright and dark fluorescent states (23). In all of our measurements, we measure the average eGFP brightness during each bin time. Therefore, our average brightness measurement depends on the equilibrium populations of the bright and dark states during the bin time of our experiments. In the following, we propose a method for calculating the eGFP brightness under the condition that the bin time is larger than the period of fluctuations between the dark and bright states.

The brightness of the eGFP bright fluorescent state was measured in vitro in a solution of eGFP in phosphate buffer,

pH 7.2, under the same laser intensity conditions as the cell membrane experiments. Under these conditions, the diffusion time of the eGFP molecules is ~80 μs, whereas the average rate of fluctuation between the dark and the bright state is >300 μs. Therefore, during the solution experiments, the observed eGFP molecules for the most part remain in the bright state throughout their passage through the detection area. Thus, the brightness of the bright state can be measured directly from solution experiments to be 11 kHz.

In contrast to the fast diffusion of eGFP in solution, the diffusion in the membrane of eGFP fused to the EGF receptor is relatively slow with a $\tau \sim 50$ ms. Therefore, during the passage of the eGFP-labeled EGF receptor through the detection volume, one sees many fluctuations between the dark and the bright state of the eGFP. Since the rate of these fluctuations is below 1 ms, they are clearly detected by the fluorescence correlation function (see Fig. 1 *B*). Here, we develop the formalism in which a superposition of fluctuations between a dark and a bright state are considered along with the diffusion process.

The rate at which molecules are pumped from the dark state D to the bright state U is k_+ and from U to D is k_-. The dynamics of the transfer between the states is governed by the following differential equations, assuming intensity independent transition rates:

$$\frac{dU}{dt} = Dk_+ - Uk_-$$
$$\frac{dD}{dt} = Uk_- - Dk_+$$

with the initial conditions of $U(0) = 1$ and $D(0) = 0$, the time dependent concentration becomes

$$U(t) = \frac{K}{1+K} + \frac{e^{-t/t_{\text{trans}}}}{1+K}$$
$$D(t) = \frac{1}{1+K} - \frac{e^{-t/t_{\text{trans}}}}{1+K}$$

in which $K = k_+/k_-$ and $1/t_{\text{trans}} = k_+ + k_-$.

The fluorescence correlation function in general can be written as

$$G(\tau) = \frac{\langle F(t)F(t+\tau)\rangle}{\langle F(t)\rangle^2}.$$

The correlation function of a system under isomerization condition has been derived in the third appendix of Elson and Magde (24) for a system fluctuating between dark and a bright state:

$$G(\tau) \propto \frac{\left(1 + fe^{-t/t_{\text{trans}}}\right)}{(1 + t/t_{\text{D}})} \qquad (11)$$
$$f = \frac{1}{K}.$$

Both f and t_{trans} can be measured by fitting Eq. 11 to the correlation functions of the receptors on the membrane.

The brightness of the GFP accompanying a membrane receptor is then derived as

$$\langle q_{\text{GFP\_Membrane}}\rangle = \frac{K}{1+K}\langle q_{\text{GFP\_Solution}}\rangle.$$

This yields a brightness of 5.5 kHz for the eGFP on the membrane.

Analysis of EGF receptor clustering using modified FIDA

eGFP-EGF receptors were stably expressed in CHO cells that do not express endogenous EGF receptors. Scatchard analysis of ^{125}I-EGF binding to these cells indicated the presence of ~66,000 receptors/cell. As is typical of the EGF receptor, Scatchard plots were curvilinear, indicative of two classes of sites: a high affinity site with a K_d of ~20 pM and a low affinity site with a K_d of ~2 nM (data not shown).

The fluorescent cells were subjected to FCS as described in Materials and Methods. Fig. 1 *A* shows the fluorescence intensity trace of eGFP-labeled EGF receptors diffusing in the plasma membrane of CHO cells at 37°C. Fluctuations in the fluorescent intensity trace are mainly due to changes in the number of eGFP-EGF receptors present within the small area illuminated by the laser beam at a given point in time.

When a labeled EGF receptor passes through the excitation volume, the photons emitted by the eGFP on that receptor are correlated with one another. When multiple EGF receptors are confined to a single cluster, the photons emitted from all receptors in that cluster are correlated. These correlations can be detected using FCS and analyzed by fitting to the autocorrelation function. A representative autocorrelation curve of the eGFP-EGF receptor is shown in Fig. 1 *B*. The curve clearly indicates the presence of two components. The fast component corresponds to the pH-dependent blinking of eGFP which occurs with a τ of ~300 μs (23). The slow component represents the diffusion of the EGF receptor and exhibits a τ of ~70 ms. From these data, a diffusion coefficient of 2.5 $\pm$ 0.6 $\times$ 10^{-9} cm^2/s can be calculated for the EGF receptor.

The fluorescence intensity trace can also be analyzed to obtain information about the brightness of the species that pass through the beam. Brightness is a quantity that depends solely on the properties of the instrument and the inherent spectroscopic properties of the fluorophores. Brightness is independent of diffusion and, in the absence of electronic interaction among fluorophores, the total molecular brightness of a cluster of fluorophores is equal to the sum of the individual molecular brightnesses. Thus, brightness quantifies the number of molecules in a group and is ideal for detecting clustering of fluorescent molecules.

To analyze the data based on brightnesses, photon count histograms were constructed from the fluorescence intensity traces and were fitted using Eqs. 8 and 10. A typical photon count histogram of the data obtained for eGFP-EGF receptor is shown in Fig. 1 *C*. The photon count histogram represents the

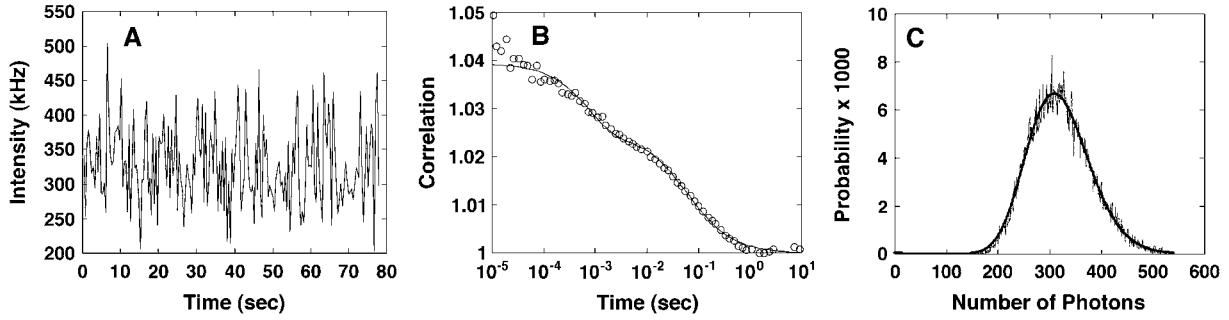

FIGURE 1 FCS and PCH of E-GFP-EGFR in CHO cell membranes. CHO cells expressing eGFP-EGF receptors were analyzed by FCS. (*A*) A typical fluorescence intensity trace. (*B*) A representative correlation function. Open circles represent actual data with only 1 in 10 data points shown to reduce crowding in the figure. The solid line represents the fit to Eq. 11 (see Materials and Methods). (*C*) A PCH of data from eGFP-EGF receptors diffusing in untreated CHO cells.

probability of detecting a certain number of photons in a fixed time period, called the bin time, during the experiment. Because the fluorescence of a cluster of molecules is directly proportional to the number of molecules in the cluster, the fluctuations of the total fluorescence detected during a bin time is highly sensitive to the presence of clusters in the experiments.

Working from the photon count histogram and following the approach developed by Kask et al. (17), our modification of FIDA utilizes inverse Fourier transforms to obtain information on the concentration of species of different brightnesses. Two key simplifications enable this analysis. First, because the EGF receptor is diffusing in the plane of the membrane, the laser profile can be well approximated by a Gaussian in the focal plane with no extension along the optical z axis. This removes complications associated with modeling the observation volume in three dimensions. Second, because it is designed to measure clustering of receptor molecules each fused to one eGFP molecule, the analysis assumes that the brightnesses of eGFP-EGF receptor clusters will be multiples of the brightness of a single eGFP molecule. In particular, for any fluorophore with brightness q, the allowed values of brightness are q, $2q$, $4q$, and $8q$. Although the allowable multiples of brightness are set, the unit brightness of the eGFP itself is not fixed during the analysis. Limiting the number of allowable values of brightness reduces the need for high photon counts per molecule to obtain accurate data. This modification results in a higher sensitivity in the analysis without requiring an increase in laser intensity that can create problems with photobleaching and phototoxicity in cells.

To determine whether the equations derived for this modified FIDA are capable of deconvoluting a known distribution of clustered fluorescent molecules, a data set was generated in silico that corresponds to a fluorophore existing as monomeric and dimeric species that are present at equal concentrations. For this analysis, monomer brightness was set to 10 counts per bin. With the bin times used in our analysis (4 ms), this would correspond to a brightness of ~2.5 kHz, which is approximately half that of the actual brightness of eGFP in our studies. As increased brightness will improve the accuracy of the data, this choice overestimates the effect of noise under our experimental conditions. Noise, associated with either 100 s of data acquisition (Fig. 2 *A*) or 10 s of data acquisition (Fig. 2 *B*), was added to the theoretical PCH curves. These theoretical data were then subjected to FIDA to generate the graphs shown in Fig. 2, *C–E*.

FIDA of the theoretical data set without added noise (Fig. 2 *C*) yields two peaks centered at 2.5 and 5 kHz. These peaks represent monomers and dimers, respectively, and are of equal size indicating equal concentrations of the monomeric and dimeric species. FIDA of the PCH to which noise had been added equivalent to that expected for 100 s of data acquisition (Fig. 2 *D*), yields a very similar result—two peaks of approximately equal size centered at 2.5 and 5 kHz. The major difference appears to be that the peak at 5 KHz is somewhat broader than that obtained using the noise-free data. Reducing the time of data acquisition to only 10 s (Fig. 2 *E*) results in insufficient sampling and hence degradation of the theoretical distribution derived from FIDA. This distribution appears to favor a monomeric species and does not accurately reflect the input brightness of the monomer. These experiments suggest that this modified FIDA can faithfully reproduce the original distribution of fluorescent species in this data set and indicate that 100 s of data acquisition yields data of sufficient quality to accurately determine the relative brightness and concentration of multiple fluorescent species in this sample. Therefore, all subsequent cellular experiments were carried out using 100 s of data acquisition.

Analysis of EGF receptor clustering using modified FIDA

CHO cells expressing eGFP-EGF receptors and maintained at 37° in balanced salt solution were imaged with a confocal microscope and a Z-scan was performed at the position of the nucleus to locate the apical and basal membranes. FCS was then performed on eGFP-EGF receptors in the apical or basal membrane and the autocorrelation curve generated (see Fig. 1 *B*). The autocorrelation function of the eGFP-EGF receptor

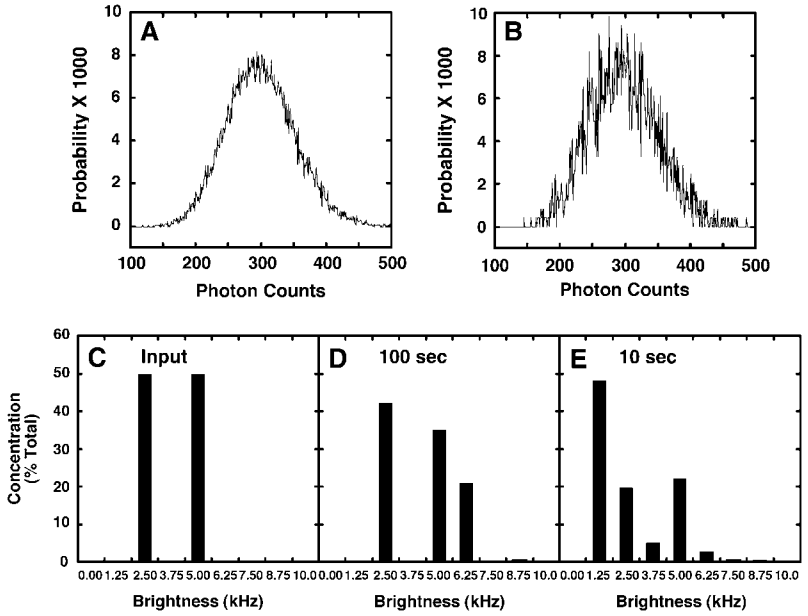

FIGURE 2 In silico error analysis of FIDA. As a test case, noisy PCH curves were generated for a system containing equal concentrations of monomer and dimer as described in Materials and Methods. These PCH curves were analyzed by FIDA to determine the distribution and brightness of the fluorescent species in the mixture. (*A*) Theoretical PCH curve including noise corresponding to 100 s of data acquisition. (*B*) Theoretical PCH curve including noise corresponding to 10 s of data acquisition. FIDA of the theoretical PCH without noise (*C*), with noise corresponding to 100 s of data acquisition (*D*), and with noise corresponding to 10 s of data acquisition (*E*).

was similar for both membranes (not shown) allowing pooling of all data sets. For each experiment, eGFP brightness was determined independently by carrying out FCS on soluble eGFP. The estimated brightness of the eGFP attached to the EGF receptor was then calculated based on the characteristics of the dark states of the eGFP as outlined above. This value was ~5.5 kHz and varied <5% among experiments.

Fig. 3 (*left panel*) shows the PCH from a FIDA analysis of data obtained from control cells. A significant concentration of species exhibited brightness centered on a value of ~5 kHz that corresponds to one GFP molecule. A lower but significant concentration of species was observed in the range of 8–12 kHz, a brightness approximately twice that of the major peak, which would represents clusters that contain two EGF receptors. A broad tail of species exhibiting brightness values between 14 and 30 kHz suggests the presence of higher order oligomers. The inset shows the total relative concentration of each size cluster. The majority of clusters (~70%) contained only one EGF receptor molecule; however, ~20% of the clusters contained two receptors. Fewer than 10% contained more than two receptors.

Although it has been demonstrated that placing two GFP molecules in tandem on a protein does not lead to detectable quenching of the GFP fluorescence (15), we assessed the effect of quenching on our FIDA analysis. To do this, a value of 20% quenching was assumed and the brightness grid was altered accordingly so that the allowable brightness values were q, $1.6q$, $3.2q$, and $6.4q$ rather than q, $2q$, $4q$, and $8q$. Data from 25 separate FCS runs from control cells were analyzed using the standard grid and the ''quenched'' grid. The results, shown in Supplemental Fig. 4, demonstrated that the introduction of quenching had relatively little effect on the resulting analysis. Together with the observation that our experimentally determined eGFP monomer brightness is very close to the calculated value for eGFP, these data suggest that quenching is not a significant problem in this system.

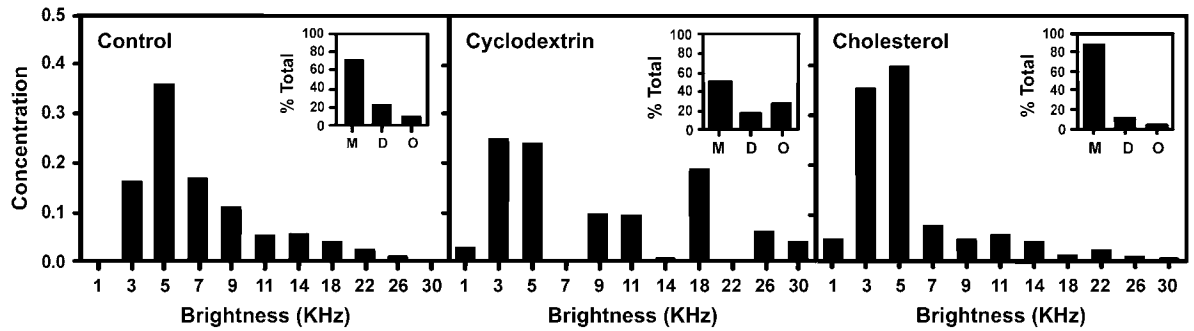

FIGURE 3 Distribution of the brightnesses of the E-GFP-EGFR in CHO cells. CHO cells expressing E-GFP-EGFR were subjected to FCS and the distribution of brightnesses determined using FIDA. (*Left panel*) Control cells. (*Middle panel*) Cholesterol-depleted cells. (*Right panel*) Cholesterol-loaded cells. The data are from pooled data sets representing 45 separate brightness measurement for controls, 45 for cholesterol-depleted, and 32 for cholesterol-loaded cells. (*Insets*) Calculated concentration of monomers (*M*), dimers (*D*), and higher order oligomers (*O*) as a percent of total species present.

The EGF receptor is known to partition into cholesterol-enriched membrane microdomains referred to as rafts (18,25–27). Since partitioning of the EGF receptor into such domains could give rise to receptor clustering, we examined the effect of cholesterol depletion on EGF receptor cluster size. CHO cells were treated with 10 mM methyl-β-cyclodextrin to extract cellular cholesterol. Assays showed that this treatment reduced cholesterol levels from 114.8 nmol/mg protein in control cells to 67.6 nmol/mg protein in the cyclodextrin-treated cells, a reduction of 41%.

FCS of EGF receptors in cholesterol-depleted cells yielded an autocorrelation function qualitatively similar to that observed in untreated cells (not shown). However, FIDA revealed significant differences from the control condition (Fig. 3, *middle panel*). As before, a major concentration of species was observed at brightness values corresponding to ~1 eGFP molecule was observed. However, there was a distinct peak of species at a brightness value of two eGFP molecules (~8–12 kHz) and the concentration of species in the region corresponding to larger clusters was significantly increased. As shown in the inset, cholesterol depletion led to a decrease in the concentration of clusters containing only a single EGF receptor (~50% in cholesterol-depleted versus ~70% in controls) and an ~3-fold increase in the concentration of clusters containing higher order oligomers (~30% in cholesterol-depleted versus ~10% in controls). Thus, the net effect of cholesterol depletion was to increase clustering of the EGF receptor.

The effect of cholesterol loading on receptor clustering was next determined. Cells were treated with cholesterol/methyl-β-cyclodextrin complexes to acutely increase cellular cholesterol before FCS. Cholesterol assays indicated that this treatment led to an increase in cholesterol content of the cells to 193.6 nmol/mg protein, or 168% of the control value.

The autocorrelation function in cholesterol-loaded cells was similar to that seen in control and cholesterol-depleted cells (not shown). However, FIDA indicated that substantial changes in EGF receptor clustering had occurred. In the brightness plot (Fig. 3, *right panel*), the concentration of clusters containing a single eGFP-EGF receptor molecule was increased as compared to untreated cells (~90% in cholesterol-loaded versus ~70% in controls). Furthermore, cholesterol loading was associated with a ~2-fold reduction in the concentration of both dimeric and higher order oligomeric species.

Effect of cholesterol depletion and repletion on EGF receptor cross-linking and signaling

The results of the FIDA analysis suggest that the EGF receptor is more highly clustered in cells depleted of cholesterol and less clustered in cells loaded with cholesterol. Chemical cross-linking of the EGF receptor was therefore used to obtain an independent assessment of the effect of cholesterol levels on receptor clustering in CHO cells. CHO cells were treated with or without EGF in the absence or presence of the cross-linking agent, BS^3. Cells were lysed and the lysates analyzed by SDS gel electrophoresis and Western blotting for EGF receptors. As shown in Fig. 4, in the absence of BS^3, the EGF receptor ran at a position that corresponded to the size of receptor monomers (~170 kDa). However, in the presence of cross-linker, higher molecular weight forms of the receptor, most likely corresponding to dimers and tetramers, were detected. As expected, addition of EGF markedly enhanced the formation of receptor dimers and tetramers under all conditions. In cyclodextrin-treated cells, basal levels of EGF receptor dimers and oligomers were 80% higher than those observed in untreated cells. Furthermore, EGF stimulation of oligomer formation was increased by ~40% compared to controls. By contrast, both basal and EGF-stimulated oligomer levels were ~50% lower in cholesterol-loaded cells than in control cells. These results suggest that cholesterol depletion enhances EGF receptor oligomerization whereas cholesterol loading inhibits oligomer formation. The findings are entirely consistent with the results of the FIDA analysis of EGF receptor clustering.

Signal transduction mediated by the EGF receptor has previously been shown to be cholesterol-dependent (19,28–30). To determine the effect of changes in cellular cholesterol content on EGF-stimulated signaling in CHO cells, the cells were depleted of or loaded with cholesterol and then stimulated with EGF. Stimulation of EGF receptor autophosphorylation was then assessed by Western blotting. As shown in Fig. 5, stimulation of cells with EGF led to an increase in the tyrosine phosphorylation of the EGF receptor in control cells. This EGF-mediated effect was substantially enhanced in cholesterol-depleted cells and markedly impaired in cholesterol-loaded cells.

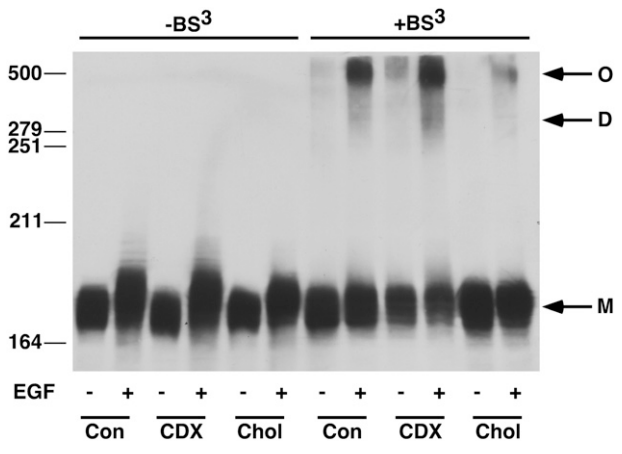

FIGURE 4 Chemical cross-linking of the EGF receptor in CHO cells. CHO cells were either depleted of or loaded with cholesterol as described in Materials and Methods. Cells were then incubated in the absence or presence of 25 nM EGF without (*lanes 1–6*) or with (*lanes 7–12*) BS^3. Lysates were analyzed by SDS gel electrophoresis and Western blotting for EGF receptors. The Western blot was intentionally overexposed to visualize the changes in levels of receptor oligomers.

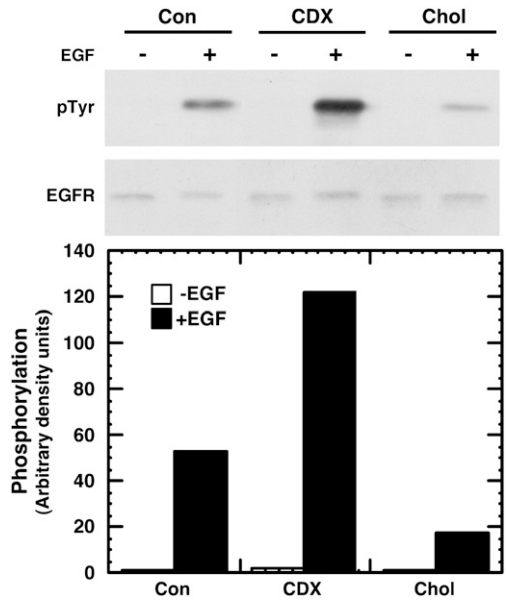

FIGURE 5 EGF receptor-mediated signaling in CHO cells. CHO cells expressing eGFP-EGF receptors were stimulated with the indicated dose of EGF for 2 min and RIPA lysates prepared. (*Top panel*) After SDS polyacrylamide gel electrophoresis, the proteins were transferred to Immobilon and were analyzed by Western blotting with the indicated antibodies. (*Bottom panel*) Quantitation of the anti-phosphotyrosine Western blots.

DISCUSSION

That the EGF receptor undergoes dimer formation upon binding EGF has been known for two decades (2). However, the extent of clustering of the receptor in either the absence or presence of EGF in intact cells has been difficult to define. Chemical cross-linking studies have produced widely varying results, a difference that could be due to differences in the cells, the cross-linking reagents used or the conditions under which the reactions were carried out (6,31). More recently, a variety of optical techniques have been applied to the study the oligomerization of the EGF receptor (7–10,32). Although these methods are more sensitive than chemical cross-linking, the technical requirements of these approaches have necessitated the use of nonphysiological conditions such as fixed or permeabilized cells and low temperatures. The use of fluorescently labeled EGF as a probe (9) avoids some of these problems but does not permit an analysis of the status of the unoccupied population of EGF receptors.

We therefore sought to develop a method to analyze the clustering of membrane proteins in live cells under physiological conditions. A cluster is defined as a group of EGF receptors that diffuse together in the cell membrane. Our goal was to develop a technique that could be generally applied to membrane proteins and would yield information on the actual distribution of proteins among clusters of a specific size, rather than simply providing the average size of clusters. We therefore turned to fluorescence brightness analysis of membrane proteins that had been tagged by fusion with a marker protein, such as eGFP.

Our analysis is similar to previous methods for brightness analysis (15–17,33), but takes advantage of two features that are unique to this EGF receptor system. First, because the EGF receptor is diffusing in the plane of the membrane, the laser profile can be well-approximated by a Gaussian in the focal plane with no extension along the optical z axis. This removes complications associated with modeling the observation volume in three dimensions. Second, because the analysis is designed to measure clustering of receptor molecules each fused to the eGFP molecule, the equations are derived for the situation in which the brightnesses of receptor clusters are multiples of the brightness of a single eGFP molecule. Limiting the number of allowable values of brightness reduces the need for high photon counts per molecule to obtain accurate data. This modification results in higher sensitivity without requiring an increase in laser intensity that can cause photobleaching and phototoxicity in cells. As a result, our modified FIDA is suitable for use in living cells and importantly, provides explicit information on the distribution of fluorescent molecules among clusters of increasing size. This provides a level of detail that has not been achieved with any previous method.

In our analysis, the brightness of the monomer is not fixed a priori because small variations in monomer brightness are expected to arise from variations in the focal point of the laser. However, the expected value of the eGFP fluorescence can be calculated based on the measurement of its photophysical properties and its observed brightness in solution. We have performed this calculation and find that the experimentally determined monomer brightness of eGFP-EGF receptor in cells is very close to the calculated value of the eGFP brightness (~5.5 kHz). This comparison provides an internal control for each experiment and the convergence of the experimental and calculated monomer brightness values is an indication of the accuracy of the analysis. This also provides a measure of how much other factors, such as quenching and optical saturation might affect the analysis. Given the agreement between theoretical and actual values of eGFP brightness observed in these experiments, the contribution of such photophysical effects appears to be minimal in this experimental setting. This is consistent with the report that expression of tandem copies of eGFP does not lead to significant fluorescence quenching (15).

The changes introduced in our modified FIDA have enabled the first explicit measurement of the distribution of clusters of eGFP-EGF receptors diffusing in the plasma membrane. Our experiments were carried out at 37°C in isotonic buffers and thus reflect the behavior of the EGF receptor under physiological conditions. The analysis suggests that the population of unstimulated EGF receptors is heterogeneous with respect to its degree of clustering. Monomers are the most common species but dimers and higher order clusters are also present. The heterogeneity of oligomerization

within the resting EGF receptor population points out the importance of utilizing a method that defines the distribution of receptors among clusters of various sizes rather than simply reporting on the average cluster size. Based on these observations, the traditional model of EGF receptor activation (2) that posits only the presence of inactive EGF monomers may need to be reformulated to include the existence of a more complex equilibrium among receptor species.

It should be noted that these data do not provide information on the nature of the EGF receptor clusters. Thus, it is not clear whether the larger clusters represent specific oligomeric forms of the EGF receptor, groups of receptors that become selectively localized in membrane microdomains or nonspecific aggregates of receptors. However, any organization of EGF receptors into preformed clusters would likely affect the ability of the receptor to dimerize upon EGF binding, making clarification of this issue a priority. It is unlikely that the clustering of the EGF receptor observed in the absence of added ligand is the result of aggregation of eGFP as it has been demonstrated that eGFP is monomeric both in solution and when anchored to a protein in the membrane (34).

Assuming that the higher order clusters contain four receptors, one can calculate an average cluster size of 1.3 receptors/cluster in untreated cells. This is smaller than the average cluster size of 2.2 receptors/cluster obtained by Clayton et al. (10) using image correlation microscopy. The difference may be due to differences in the concentration of receptors or the conditions under which the measurements were taken (live cells versus fixed cells), particularly since the fixation of the cells could lead to the artificial production of receptor dimers. Alternatively, FCS and FIDA measure only the mobile population of receptors whereas image correlation microscopy captures both the mobile and immobile populations. If immobile EGF receptors are highly clustered this would affect the calculated average extent of clustering.

Treatment of cells with EGF at 37°C is known to induce rapid internalization of the receptor. Because the time required to take FCS measurements is slow relative to receptor internalization, it was not possible to examine the effect of ligand on receptor clustering. This question will need to be addressed in a system in which the conditions have been modified to preclude receptor internalization. Because EGF receptor-mediated signaling has been shown to be affected by changes in cellular cholesterol content (19,28–30), we chose instead to examine the effect of this variable on receptor clustering.

FIDA of EGF receptors in cells that had been acutely depleted of cholesterol by treatment with methyl-β-cyclodextrin demonstrated that the equilibrium distribution of EGF receptors among clusters shifted markedly toward a more highly clustered state. Conversely, in cells that had been loaded with additional cholesterol, FIDA indicated a shift to a distribution that favored monomeric species over dimers and higher order oligomers.

The EGF receptor has been shown to be localized to cholesterol-rich, membrane microdomains known as rafts (18,26,30,35). The observation that changes in cellular cholesterol levels lead to alterations in EGF receptor clustering suggests that receptor clustering may be affected by its partitioning into these microdomains. Cholesterol loading may induce the formation of more rafts into which the EGF receptor can partition, decreasing overall clustering. Conversely, cholesterol depletion may result in the formation of fewer membrane rafts, thereby promoting clustering by concentrating EGF receptors in a smaller number of residual rafts. It is also possible that changes in cholesterol levels could affect receptor-receptor interactions making oligomerization or aggregation more or less likely. Regardless of the mechanism, it is clear that altering cellular cholesterol content leads to alterations in the equilibrium for clustering of the EGF receptor.

To independently assess the clustering of the EGF receptor in cells, chemical cross-linking of the receptor was employed. This technique has been used previously to demonstrate the dimerization of the EGF receptor in response to hormone (36). Here we showed that cholesterol depletion enhanced the formation of EGF receptor oligomers whereas cholesterol loading reduced oligomer formation. These studies provide additional evidence that EGF receptor clustering is regulated by cholesterol levels and confirm the results of the FIDA analysis.

The changes in receptor clustering documented by FIDA were associated with changes in the level of EGF-stimulated receptor autophosphorylation. Cholesterol depletion led to enhanced clustering and increased EGF-stimulated receptor autophosphorylation. Conversely, increases in cellular cholesterol levels reduced the extent of receptor clustering and were associated with a decrease in hormone-stimulated receptor autophosphorylation. These observations suggest that signaling is positively correlated with EGF receptor clustering. Receptor clustering may enhance the ability of EGF to activate the receptor population, particularly if lateral signaling among receptors is part of the activation mechanism (32,37). The finding that EGF receptor clustering, and possibly signaling, can be regulated by manipulating the lipid composition of the membrane reveals an unexpected level of complexity in the control of signaling via this receptor.

Dimerization (2), and possibly tetramerization (10,38), play a role in the activation of the EGF receptor tyrosine kinase. It is therefore important to develop methods that allow the assessment of receptor clustering in intact cells so that the role of receptor oligomerization in the activation of the EGF receptor can be accurately determined. This modified form of FIDA offers a new approach to the study of EGF receptor activation in situ in living cells.

SUPPLEMENTARY MATERIAL

To view all of the supplemental files associated with this article, visit www.biophysj.org.

The authors thank Mr. Thomas Stump for assistance with the FCS instrumentation.

This work was supported by National Institutes of Health grants RO1 GM064491 (LJP) and AR047591 (ELE).

REFERENCES

1. Ullrich, A., L. Coussens, J. S. Hayflick, T. J. Dull, A. Gray, A. W. Tam, J. Lee, Y. Yarden, T. A. Libermann, J. Schlessinger, J. Downward, E. L. V. Mayes, N. Whittle, N. D. Waterfield, and P. H. Seeburg. 1984. Human epidermal growth factor receptor cDNA sequence and aberrant expression of the amplified gene in A431 epidermoid carcinoma cells. *Nature.* 309:418–425.
2. Yarden, Y., and J. Schlessinger. 1987. Epidermal growth factor induces rapid, reversible aggregation of the purified epidermal growth factor receptor. *Biochem.* 26:1443–1451.
3. Ferguson, K. M., M. B. Berger, J. M. Mendrola, H.-S. Cho, D. J. Leahy, and M. A. Lemmon. 2003. EGF activates its receptor by removing interactions that autoinhibit ectodomain dimerization. *Mol. Cell.* 11:507–517.
4. Garrett, T. P. J., N. M. McKern, M. Lou, T. C. Elleman, T. E. Adams, G. O. Lovrecz, H.-J. Zhu, F. Walker, M. J. Frenkel, P. A. Hoyne, R. N. Jorissen, E. C. Nice, A. W. Burgess, and C. W. Ward. 2002. Crystal structure of a truncated epidermal growth factor receptor extracellular domain bound to transforming growth factor α. *Cell.* 110:763–773.
5. Ogiso, H., R. Ishitani, O. Nureki, S. Fukai, M. Yamanaka, J.-H. Kim, K. Saito, A. Sakamoto, M. Inoue, M. Shirouzu, and S. Yokoyama. 2002. Crystal structure of the complex of human epidermal growth factor and receptor extracellular domains. *Cell.* 110:775–787.
6. Moriki, T., H. Maruyama, and I. N. Maruyama. 2001. Activation of preformed EGF Receptor dimers by ligand-induced rotation of the transmembrane domain. *J. Mol. Biol.* 311:1011–1026.
7. Gadella, T. W. J., and T. M. Jovin. 1995. Oligomerization of epidermal growth factor receptors on A431 cells studied by time-resolved fluorescence imaging microscopy. a stereochemical model for tyrosine kinase receptor activation. *J. Cell Biol.* 129:1543–1558.
8. Martin-Fernandez, M., D. T. Clarke, M. J. Tobin, S. V. Jones, and G. R. Jones. 2002. Preformed oligomeric epidermal growth factor receptors undergo and ectodomain structure change during signaling. *Biophys. J.* 82:2415–2427.
9. Sako, Y., S. Minoguchi, and T. Yanagida. 2000. Single-molecule imaging of EGFR signalling on the surface of living cells. *Nat. Cell Biol.* 2:168–172.
10. Clayton, A. H. A., F. Walker, S. G. Orchard, C. Henderson, D. Ruchs, J. Rothacker, E. C. Nice, and A. W. Burgess. 2005. Ligand-induced dimer-tetramer transition during the activation of cell surface epidermal growth factor receptor. a multidimensional microscopy analysis. *J. Biol. Chem.* 280:30392–30399.
11. Palmer, A. G., 3rd, and N. L. Thompson. 1987. Molecular aggregation characterized by high order autocorrelation in fluorescence correlation spectroscopy. *Biophys. J.* 52:257–270.
12. Qian, H., and E. L. Elson. 1990. Distribution of molecular aggregation by analysis of fluctuation moments. *Proc. Natl. Acad. Sci. USA.* 87: 5479–5483.
13. Chen, Y., J. D. Muller, Q. Ruan, and E. Gratton. 2002. Molecular brightness characterization of EGFP in vivo by fluorescence fluctuation spectroscopy. *Biophys. J.* 82:133–144.
14. Chen, Y., J. D. Muller, P. T. So, and E. Gratton. 1999. The photon counting histogram in fluorescence fluctuation spectroscopy. *Biophys. J.* 77:553–567.
15. Chen, Y., L.-N. Wei, and J. D. Muller. 2003. Probing protein oligomerization in living cells with fluorescence fluctuation spectroscopy. *Proc. Natl. Acad. Sci. USA.* 100:15492–15497.
16. Chen, Y., L.-N. Wei, and J. D. Muller. 2005. Unraveling protein-protein interactions in living cells with fluorescence fluctuation brightness analysis. *Biophys. J.* 88:4366–4377.
17. Kask, P., K. Palo, D. Ullmann, and K. Gall. 1999. Fluorescence-intensity distribution analysis and its application in biomolecular detection technology. *Proc. Natl. Acad. Sci. USA.* 96:13756–13761.
18. Pike, L. J., and J. M. Miller. 1998. Cholesterol depletion de-localizes PIP_2 and inhibits hormone-stimulated phosphatidylinositol turnover. *J. Biol. Chem.* 273:22298–22304.
19. Westover, E. J., D. F. Covey, H. L. Brockman, R. E. Brown, and L. J. Pike. 2003. Cholesterol depletion results in site-specific increases in EGF receptor phosphorylation due to membrane level effects: studies with cholesterol enantiomers. *J. Biol. Chem.* 278:51125–51133.
20. Saffarian, S., and E. L. Elson. 2003. Statistical analysis of fluorescence correlation spectroscopy: the standard deviation and bias. *Biophys. J.* 84:2030–2042.
21. Wohland, T., R. Rigler, and H. Vogel. 2001. The standard deviation in fluorescence correlation spectroscopy. *Biophys. J.* 80:2987–2999.
22. Inoue, M. 2004. Partitioning of NaPi cotransporter in cholesterol-, sphingomyelin-, and glycosphingolipid-enriched membrane domains modulates NaPi protein diffusion, clustering, and activity. *J. Biol. Chem.* 279:49160–49171.
23. Haupts, U., S. Maiti, P. Schwille, and W. W. Webb. 1998. Dynamics of fluorescence fluctuations in green fluorescent protein observed by fluorescence correlation spectroscopy. *Proc. Natl. Acad. Sci. USA.* 95: 13573–13578.
24. Elson, E. L., and D. Magde. 1974. Fluorescence correlation spectroscopy. *Biopolymers.* 13:1–27.
25. Smart, E. J., Y.-S. Ying, C. Mineo, and R. G. W. Anderson. 1995. A detergent-free method for purifying caveolae membrane from tissue culture cells. *Proc. Natl. Acad. Sci. USA.* 92:10104–10108.
26. Mineo, C., G. L. James, E. J. Smart, and R. G. W. Anderson. 1996. Localization of epidermal growth factor-stimulated ras/raf-1 interaction to caveolae membrane. *J. Biol. Chem.* 271:11930–11935.
27. Waugh, M. G., D. Lawson, and J. J. Hsuan. 1999. Epidermal growth factor receptor activation is localized within low-buoyant density, non-caveolar membrane domains. *Biochem. J.* 337:591–597.
28. Pike, L. J., and L. Casey. 2002. Cholesterol levels modulate EGF receptor-mediated signaling by altering receptor function and trafficking. *Biochem.* 41:10315–10322.
29. Ringerike, T., F. D. Glystad, F. O. Levy, I. H. Madshus, and E. Stang. 2002. Cholesterol is important in control of egf receptor kinase activity but EGF receptors are not concentrated in caveolae. *J. Cell Sci.* 115:1331–1340.
30. Roepstorff, K., P. Thomsen, K. Sandvig, and B. van Deurs. 2002. Sequestration of EGF Receptors in non-caveolar lipid rafts inhibits ligand binding. *J. Biol. Chem.* 277:18954–18960.
31. Yu, X., K. D. Sharma, T. Takahashi, R. Iwamoto, and E. Mekada. 2002. Ligand-independent dimer formation of epidermal growth factor receptor (EGFR) Is a Step Separable from ligand-induced EGFR signaling. *Mol. Biol. Cell.* 13:2547–2557.
32. Verveer, P. J., F. S. Wouters, A. R. Reynolds, and P. I. H. Bastiaens. 2000. Quantitative imaging of lateral ErbB1 receptor signal propagation in the plasma membrane. *Science.* 290:1567–1570.
33. Kask, P., K. Palo, N. Fay, L. Brand, U. Mets, D. Ullmann, J. Jungmann, J. Pschorr, and K. Gall. 2000. Two-dimensional fluorescence intensity distribution analysis: theory and applications. *Biophys. J.* 78:1703–1713.
34. Sharma, P., R. Varma, R. C. Sarasij, K. Gousset, G. Krishnamoorthy, M. Rao, and S. Mayor. 2004. Nanoscale organization of multiple GPI-anchored proteins in living cell membranes. *Cell.* 116:577–589.
35. Mineo, C., G. N. Gill, and R. G. W. Anderson. 1999. Regulated migration of epidermal growth factor receptor from caveolae. *J. Biol. Chem.* 274:30636–30643.
36. Kuppuswamy, D., and L. J. Pike. 1991. Desensitization of the EGF receptor alters its ability to undergo EGF-induced dimerization. *Cell. Signal.* 3:107–117.
37. Ichinose, J., M. Murata, T. Yanagida, and Y. Sakao. 2004. EGF signaling amplification induced by dynamic clustering of EGFR. *Biochem. Biophys. Res. Commun.* 324:1143–1149.
38. Whitson, K. B., J. M. Beechem, A. H. Beth, and J. V. Staros. 2004. Preparation and characterization of Alexa Fluor 594-labeled epidermal growth factor for fluorescence resonance energy transfer studies: application to the epidermal growth factor receptor. *Anal. Biochem.* 324:227–236.